[9] G. D. Smith, *Numerical Solution of Partial Differential Equations*. Oxford, U.K.: Oxford Univ. Press, 1978.

[10] M. B. Monagan and J. S. Devitt, *Maple V Programming Guide*. New York: Springer-Verlag, 1978.

[11] E. I. Jury, *Inners and Stability of Dynamic Systems*. New York: Wiley, 1974.

[12] D. M. Pozar, *Microwave Engineering*. Reading, MA: Addison-Wesley, 1990.

[13] P. H. Harms, J.-F. Lee, and R. Mittra, "A study of nonorthogonal FDTD method versus the conventional FDTD technique for computing resonant frequencies of cylindrical cavities," *IEEE Trans. Microwave Theory Tech.*, vol. 41, pp. 668–676, May 1993.

Hybrid Planar NRD-Guide Magic-Tee Junction

Yves Cassivi and Ke Wu

***Abstract*—A new magic-tee circuit is proposed and developed, which is based on the hybrid integration technology of a planar and nonradiative dielectric (NRD) guide. The magic-tee junction combines an NRD-guide T-junction with a microstrip T-junction. Furthermore, LSM_{10}-mode radiators are introduced in the magic-tee circuit to reduce its resonance problem. Measured results show that an isolation of 20 dB can easily be achieved between the sum and difference ports.**

***Index Terms*—Hybrid planar/nonradiative dielectric (NRD) guide technology, magic-tee junction, millimeter-wave technology, mode suppressor, nonradiative dielectric (NRD) waveguide.**

I. Introduction

The nonradiative dielectric (NRD) waveguide is a promising technology for millimeter-wave applications. Various types of NRD-guide components have been proposed and developed [1], including filters, couplers, antennas, and hybrid planar NRD circuits [2]. In the latter case, the NRD-guide is coupled to a planar structure, e.g., a microstrip line, thereby combining and deploying the advantages of each individual design platform. However, there are no NRD-guide-based magic-tee junctions reported thus far in the literature. We propose a magic-tee junction that uses an NRD-guide T-junction combined with a microstrip T-junction.

In an NRD-guide, the two fundamental hybrid modes are the LSE_{10} and LSM_{10} modes. The LSM_{10} mode is usually preferred because it has a low-loss transmission property and it is the dominant TM_y-type mode, while the LSE_{10} mode is the second TE_y mode after the LSE_{00} mode. Mode conversion between the LSE_{10} and LSM_{10} modes is omnipresent in NRD-guide bends [3] and misalignments [4]. Yoneyama *et al.* [3] have developed a useful relationship between the radius of bend and the conversion loss for the LSM_{10} mode. This analysis shows that, for a very sharp bend, the LSM_{10} mode can almost completely be converted into its LSE_{10} counterpart. For this reason, the development of NRD-guide T-junctions [5]–[7] has led to a topology that was optimized for the complete modal conversion of an LSM_{10}-mode input signal into two equal LSE_{10}-mode signals at the output ports. It was also shown that a T-junction splitting an LSE_{10} mode into two LSM_{10} signals is also feasible [7]. A useful property of that type of NRD-guide T-junctions is the phase difference between the two outputs. Due to the electromagnetic field configuration of the LSE_{10} and LSM_{10} modes, an LSM_{10}-to-LSE_{10}-mode conversion T-junction will have 180° phase difference between the two outputs, but an LSE_{10}-to-LSM_{10}-mode conversion T-junction will have 0° phase difference between the two outputs. This is equivalent to the E- and H-plane rectangular waveguide T-junctions. Since the microstrip T-junction has an in-phase output signal, the NRD-guide LSM_{10}-to-LSE_{10}-mode conversion T-junction is adopted for the proposed magic-tee junction.

Manuscript received July 31, 2001; revised January 8, 2002.

The authors are with the Poly-Grames Research Center, École Polytechnique de Montréal, Montréal, QC, Canada H3V 1A2 (e-mail: cassivy@grmes.polymtl.ca).

Digital Object Identifier 10.1109/TMTT.2002.803451.

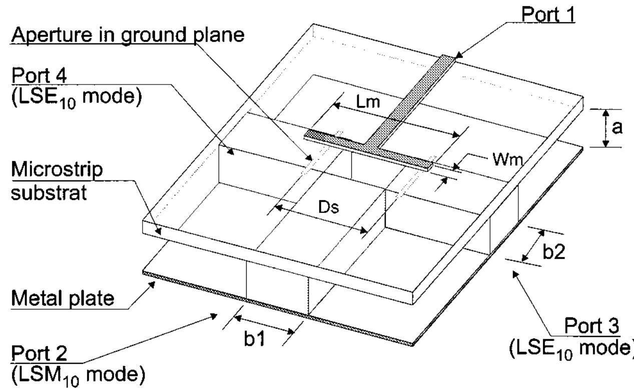

Fig. 1. Hybrid planar/NRD-guide magic-tee junction topology.

In this paper, a practical hybrid planar/NRD-guide magic tee is described first and then analyzed. It is shown that a resonance problem within the magic-tee junction appears when microstrip-to-NRD-guide transitions are placed at the three NRD-guide ports of the magic tee. Thus, an LSM_{10}-mode load is introduced to resolve this problem. The load does not affect the LSE_{10} mode and its construction is compatible with the hybrid planar/NRD-guide technology. Simulation and measurement results for the proposed magic tee are presented.

II. Hybrid Planar/NRD-Guide Magic-Tee Junction

The proposed magic-tee junction topology consists of an NRD-guide T- junction combined with a planar junction. The first option is to use a microstrip T-junction that has in-phase outputs with an NRD-guide LSM_{10}-to-LSE_{10} T-junction. The second approach is to use an NRD-guide LSE_{10}-to-LSM_{10} T-junction with a slotline-to-microstrip-line T-junction, the later having out of phase outputs. Only the first option is studied in this paper.

A. Proposed Topology for the NRD Magic-Tee Junction

Fig. 1 shows the proposed topology. The new magic tee is composed of an NRD-guide LSM_{10}-to-LSE_{10} T-junction, which is used as a difference port, and a microstrip junction used as a sum port. The microstrip T-junction and NRD-guide T-junction are combined with two microstrip-to-NRD-guide LSE_{10}-mode transitions [8]. The two transitions are placed over the two output branches of the NRD-guide T-junction. This arrangement produces two in-phase LSE_{10}-mode signals inside the output branches of the NRD-guide T-junction. Since two such signals are in phase, they cannot produce an LSM_{10}-mode signal at the difference port, contributing to a good isolation of the sum and difference ports. Similarly, the out-of-phase LSE_{10}-mode output signals produced by the NRD-guide T-junction generate a virtual short

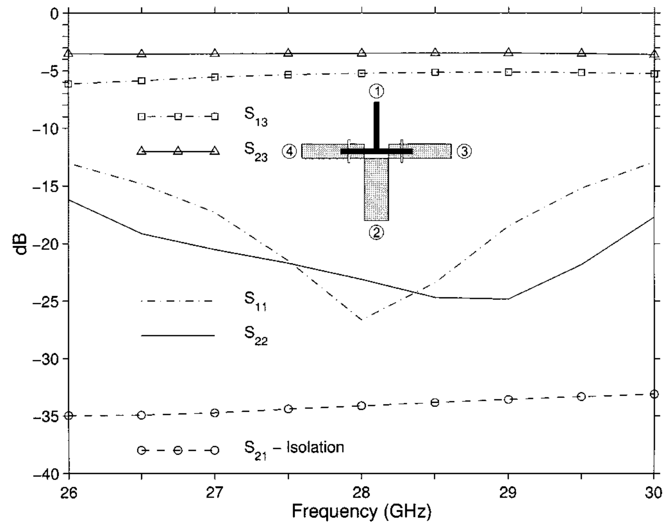

Fig. 2. Simulated results of the hybrid planar/NRD-guide magic-tee junction.

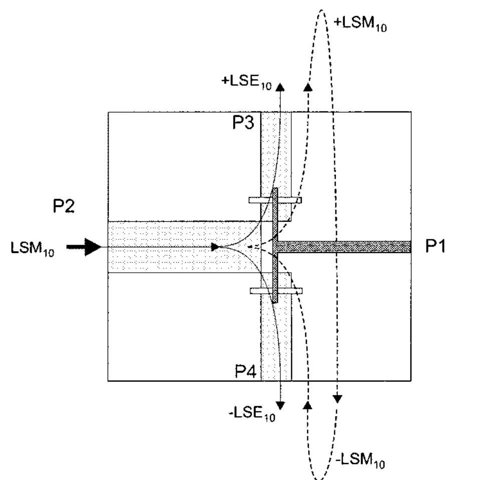

(a)

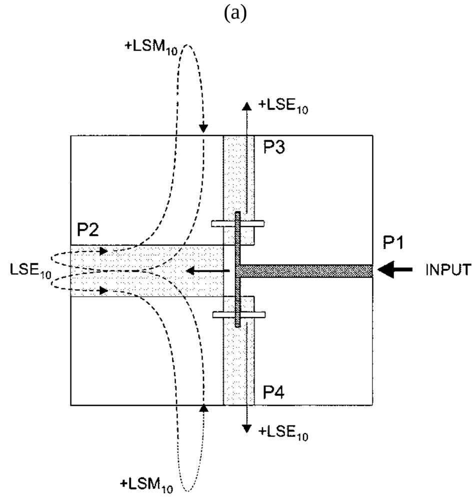

(b)

Fig. 3. Resonance paths in the hybrid NRD-guide magic-tee junction. (a) Resonance path for port 2 with an LSM_{10} mode input signal. (b) Resonance path for port 1.

circuit at the center of the microstrip T-junction of the sum port, which also contributes to a good isolation between the two ports.

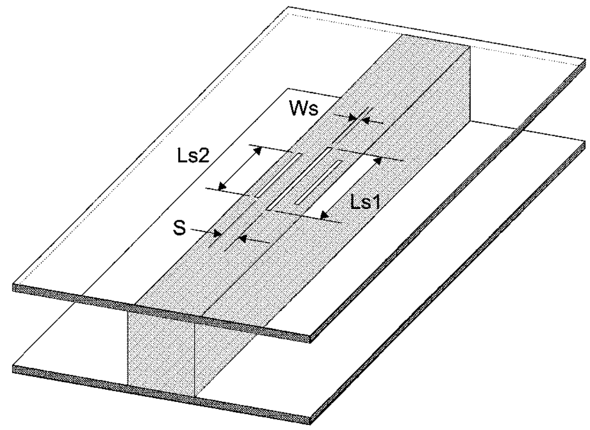

Fig. 4. NRD-guide LSM_{10}-mode load topology.

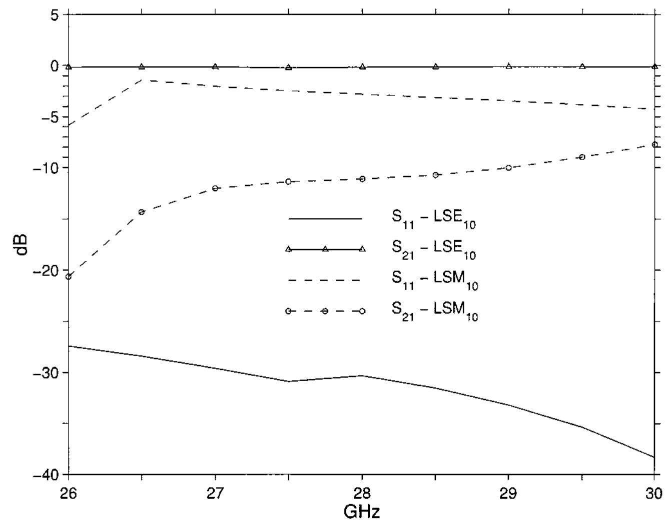

Fig. 5. Simulated results for the LSM-mode load.

B. Design Procedure

The design of the magic tee is carried out in two stages. In the first stage, the NRD-guide LSM_{10}-to-LSE_{10} T-junction is optimized for the frequency band of interest. In our case, this frequency band is 27-29 GHz. Polystyrene material with a dielectric constant of 2.4 is used. The resulting dimensions of the junction (see Fig. 1) are $a = 4.953$ mm, $b_1 = 4.064$ mm and $b_2 = 3.302$ mm. The second stage is the optimization of the microstrip junction combined with the NRD-guide T-junction. This optimization is performed on the aperture size and position of the two transitions, as well as on the linewidth of the microstrip T-junction (see Fig. 1). The results of the optimization are $Ds = 6.098$ mm, $Lm = 9.652$ mm, and $Wm = 0.61$ mm. The ground slots have a length of 6.1 mm and a width of 0.508 mm. The simulated results of the overall hybrid planar NRD-guide magic-tee junction are presented in Fig. 2. Note that the difference between S_{31} and S_{32} is caused by the insertion loss of the two microstrip-to-NRD-guide LSE_{10}-mode transitions (which is around 1.5 dB), which only affect port 1.

To measure the proposed magic tee, appropriate microstrip-to-NRD-guide transitions are added to ports 2–4. However, a resonance problem takes place because of these transitions.

C. Resonance Problem

A number of spikes were noticeable in the measurement and simulation results of the magic-tee junction when transitions are

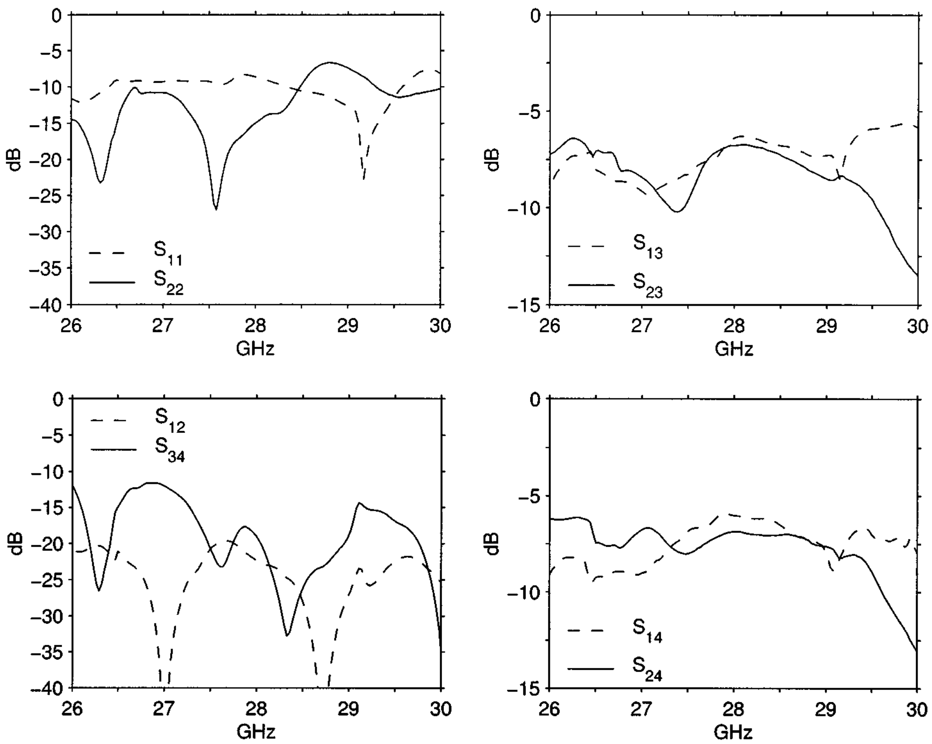

Fig. 6. Measurement results for the complete hybrid magic-tee junction that includes LSM_{10}-mode loads and microstrip-to-NRD-guide transitions.

introduced. They are similar to the case in which spikes appear when an NRD-guide bend is terminated by LSM_{10}-mode waveguide transitions. As explained by Yoneyama *et al.* [3], this construction results in an LSE_{10}-mode cavity having resonance at discrete frequencies. At resonance, the LSE_{10}-mode signal, which is linked to the LSM_{10}-mode signal through the mode conversion, cannot propagate in the structure, resulting in a high insertion loss for the LSM_{10} mode at these frequencies. In the hybrid NRD-guide magic tee, the spikes present in the results for S_{11} are at different frequencies compared with those present in the results for S_{22}. This indicates that two separate resonance mechanisms (or cavities) exist in the structure. One is associated with port 1, while the other is related to port 2.

Fig. 3 illustrates the two mechanisms. In the first case [see Fig. 3(a)], an LSM_{10}-mode signal is injected into port 2. This produces out-of-phase LSE_{10} signals at $P3$ and $P4$. Also, since not all of the input signals are converted, out-of-phase LSM_{10} signals are also present at $P3$ and $P4$. The LSE_{10}-type microstrip-to-NRD-guide transitions placed at $P3$ and $P4$ will completely reflect the LSM_{10} signals. In the way back to the NRD-guide T-junction, a small portion of the out-of-phase LSM_{10} signals will go back to port 2, but most of it will be trapped inside the output branches. Thus, in this case, the two output branches of the NRD T-junction form a cavity.

In the second case [see Fig. 3(b)], an input signal at port 1 will produces in-phase LSE_{10} signals at $P3$ and $P4$. However, it will also give some LSE_{10}-mode signal leakage at $P2$. This signal is reflected back by the LSM_{10}-mode microstrip-to-NRD-guide transition. Coming back to the NRD-guide T-junction, the LSE_{10} signal is split in two in-phase LSM_{10} signals at $P3$ and $P4$. The LSE_{10}-type transitions present at the output ports will reflect those LSM_{10} signals. They will come back again in the NRD-guide T-junction to generate an LSE_{10}-mode signal at $P2$ so as to close the loop. As such, the cavity is, in this case, the entire NRD T-junction.

The above analysis indicates that placing an LSE_{10}-mode suppressor [10], [11] at the end of the main branch of the NRD-guide T-junction (port 1) will not remove the spikes because it will not affect the resonance path of port 2 [see Fig. 3(a)], but would resolve the resonance path of port 1. The only common factor of the two resonances is the presence of LSM_{10}-mode signals at $P3$ and $P4$. Thus, if LSM_{10}-mode loads are placed at $P3$ and $P4$ with sufficient attenuation, the two resonance problems could be removed.

III. LSM_{10}-Mode Load

The proposed LSM_{10}-mode load is made of small longitudinal ground apertures over the dielectric slab of the NRD-guide, as shown in Fig. 4. Note that the same apertures could be copied on the bottom ground plate of the NRD-guide, making the suppressor more effective because of its symmetry. However, it is not necessary in our application. The working principle of this load can be explained as follows. Since the LSM_{10} mode only has magnetic fields in the longitudinal plane of the NRD-guide, longitudinal slot in the metallic plates will have optimum interaction with the LSM_{10} mode. The impedance of the load is both resistive and reactive, providing both radiation and reflection losses. The radiation loss attenuates the signal and the reflection loss reduces the length of the cavity, as explained in the previous section. Two different aperture lengths are used to improve the frequency bandwidth. Since the current density of the LSE_{10} mode is mostly longitudinal, it will not be noticeably affected by the longitudinal ground apertures. Note that, because the apertures of the LSM_{10}-mode load are longitudinal, they will not be coupled with the transversal aperture of the LSE_{10}-mode microstrip-to-NRD-guide transitions of port 1, but it could interfere with the LSM_{10}-mode transition of port 2.

Our goal is to optimize the load so it can provide a sufficient attenuation in the frequency band of interest. The obtained dimensions for the ground apertures are $Ls1 = 4.064$ mm, $Ls2 = 3.556$ mm, $S = 1.524$ mm, and $Ws = 0.254$ mm. The simulated results for the load are presented in Fig. 5, indicating a minimum attenuation level of 8 dB achievable over the bandwidth. It is also shown that the circuit does not affect the transmission of the LSE_{10} mode.

Fig. 6 gives measurement results of the proposed magic-tee junction with LSM_{10}-mode loads and microstrip-to-NRD-guide transitions. The NRD-guide magic tee was constructed using our developed engraved nonradiative dielectric (ENRD) fabrication technique [9]. It shows that no spikes are noticeable, except at 29.2 GHz, where the spike may be caused by a parasitic mode. The insertion level of S_{13}, S_{23}, S_{14}, and S_{24} are high because of the added transitions in ports 2–4, which increase the insertion loss of the transmission coefficients associated with port 2 (S_{23} and S_{24}) by approximately 2.7 dB and add approximately 1.2 dB for S_{13} and S_{14}. These estimations are based on measurement results of the microstrip-to-NRD transitions taken from previous studies [8], [9]. Also note that improvement is needed in the matching of the microstrip-to-NRD transitions. This would considerably improve the performance of the magic tee, especially for the S_{13}-, S_{23}-, S_{14}-, and S_{24}-parameters.

IV. Conclusion

A new class of hybrid microstrip/NRD-guide magic-tee junctions has been proposed and developed. Simulated and measured results have shown the operating mechanism and preliminary performance of the hybrid microstrip/NRD-guide magic tee. Amplitude unbalance of ports 1 and 2 with respect to transmission characteristics has been discussed. An LSM_{10}-mode attenuator has been developed for this magic tee so as to resolve resonance problem in the circuit when microstrip-to-NRD-guide transitions are added at the three NRD ports.

References

[1] T. Yoneyama, "Millimeter-wave integrated circuits using nonradiative dielectric waveguide," *Electron. Commun. Jpn.*, pt. 2, vol. 74, no. 2, pp. 20–28, 1991.

[2] K. Wu and L. Han, "Hybrid integrated technology of planar circuits and NRD guide for cost effective microwave and millimeter-wave applications," *IEEE Trans. Microwave Theory Tech.*, vol. 45, pp. 946–954, June 1997.

[3] T. Yoneyama, H. Tamaki, and S. Nishida, "Analysis and measurement of nonradiative dielectric waveguide bends," *IEEE Trans. Microwave Theory Tech.*, vol. MTT-34, pp. 876–882, Aug. 1986.

[4] F. Boone and K. Wu, "Mode conversion and design consideration of integrated nonradiative dielectric (NRD) components and discontinuities," *IEEE Trans. Microwave Theory Tech.*, vol. 48, pp. 482–492, Apr. 2000.

[5] T. Yoneyama and S. Nishida, "Nonradiative dielectric waveguide T-junctions for millimeter-wave applications," *IEEE Trans. Microwave Theory Tech.*, vol. MTT-33, pp. 1239–1241, Nov. 1985.

[6] Y. Endo and T. Yoneyama, "Finite element analysis of discontinuities in nonradiative dielectric waveguide," *Electron. Commun. Jpn.*, pt. 2, vol. 72, no. 11, pp. 102–112, 1989.

[7] F. Kuroki and T. Yoneyama, "NRD-guide center-fed H-shaped five port at millimeter-wave-lengths," in *Proc. 3rd Asia–Pacific Microwave Conf.*, Tokyo, Japan, 1990, pp. 7–10.

[8] A. Bacha and K. Wu, "LSE-mode balun for hybrid integration of NRD-guide and microstrip line," *IEEE Microwave Guided Wave Lett.*, vol. 8, pp. 199–201, May 1998.

[9] Y. Cassivi, D. Deslandes, and K. Wu, "Engraved NRD-guide for millimeter-wave integrated circuits," in *IEEE MTT-S Int. Microwave Symp. Dig.*, vol. 2, June 2000, pp. 605–608.

[10] H. Yoshinaga and T. Yoneyama, "Design and fabrication of a nonradiative dielectric waveguide circulator," *IEEE Trans. Microwave Theory Tech.*, vol. 36, pp. 1526–1529, Nov. 1988.

[11] J. Huang, K. Wu, F. Kuroki, and T. Yoneyama, "Computer-aided design and optimization of NRD-guide mode suppressors," *IEEE Trans. Microwave Theory Tech.*, vol. 44, pp. 905–910, Nov. 1996.